

Effect of Molybdenum Trioxide in the Behavior of Poly(vinyl alcohol) Nanocomposites Systems Focusing New Systems for Protection against COVID-19

Maria Inês Bruno Tavares*, José Carlos Dutra Filho, Tais Nascimento, Gisele Cristina Valle Iulianelli and Pedro Paulo Merat

Instituto de Macromoléculas Professora Eloisa, Universidade Federal do Rio de Janeiro, Centro de Tecnologia, Bloco J, Cidade Universitária, Ilha do Fundão, CP 68525, Rio de Janeiro, RJ, 21945-970, Brazil

Abstract: The purpose of this work was to study the molecular dynamics, morphology, mechanical and thermal performance of nanomaterials formed by poly(vinyl alcohol) and molybdenum trioxide (PVA/MoO₃) obtained through solution casting method, focusing new materials with therapeutic applications since the molybdenum trioxide exhibit an excellent antibacterial activity and could be a pathway to prevent viruses. The obtaining materials were characterized by conventional techniques as X-ray diffraction, thermogravimetric and dynamical-mechanical analysis. The unconventional low-field NMR relaxometry was used to evaluate the molecular dynamic and morphology of these systems. The results obtained showed that the MoO₃ addition into PVA matrix promote an increase on the thermal stability at higher temperatures and a progressive increase on the rigidity of the PVA systems. Also changes in the molecular mobility of nanomaterials determined through the proton spin-lattice relaxation time showed that low proportion of molybdenum trioxide increased the intercalation of the poly(vinyl alcohol) chains between oxide lamellae while higher quantity of molybdenum trioxide caused an inverse effect on the oxide lamellae delamination. From those results the nanomaterials presented a mixed structural organization as intercalated and exfoliated morphologies. According to these first results, the nanocomposites obtained promise to be antimicrobial and antiviral agent to prevent COVID-19 and similar viruses.

Keywords: COVID-19, molybdenum trioxide, PVA, nanocomposites, NMR relaxation.

INTRODUCTION

Molybdenum trioxide (MoO₃) is a layered compound that appears naturally, but rarely as the mineral molybdite and it is also a compound produced on the largest scale. This oxide is normally employed as an oxidation catalyst and as a raw material for the production of molybdenum metal and recently it was reported that the molybdenum oxides exhibit an extraordinary antibacterial activity [1-4].

Extensive studies have suggested that highly active metal and metal oxide exhibit excellent antimicrobial properties. However, these materials show several drawbacks limiting their applicability such as a low active surface area, low durability and a possible high cytotoxicity [5]. An alternative to solve these issues is the incorporation of these materials into polymer matrices, since polymers can help disperse particles, leading to increase surface area, increasing durability by coating particles and make them more biocompatible if an appropriate matrix and preparation method are employed. Several researches investigated the antimicrobial characteristics or properties of metal and metal oxides particles or nanoparticle, such as Ag,

Cu, Au, TiO₂, ZnO, MgO and CuO, when they are incorporated in polymer matrices [6-14].

Nanotechnology has been a very promising alternative in the area of polymers for promoting exceptional results such as in the increase performance of nanocomposites. However, so far, rare studies involve the use of molybdenum trioxide to obtain polymer nanocomposites with specific characteristics. The use of metal oxides to obtain nanomaterials for a diversity of application has been increased in the last few years, due to the rapid development of the nanotechnology area and our group has been investigating different systems formed by synthetic and natural polymers and metal oxides [15-21].

After obtaining nanomaterials, their characterization has a great importance to present and understand their properties and to infer in the final application of these materials [15-22]. Several techniques must be used to really characterize the nanomaterials due to their particular organization and, of course, to the final morphology adopted after nanoparticles incorporation in the polymer matrix. It is possible to divide them in conventional ones and specific ones, in the last class nuclear magnetic resonance is the best technique that can be applied [23-30].

In this work, solution casting mode was chosen as a technique to disperse molybdenum trioxide into PVA

*Address correspondence to this author at the Instituto de Macromoléculas Professora Eloisa, Universidade Federal do Rio de Janeiro, Centro de Tecnologia, Bloco J, Cidade Universitária, Ilha do Fundão, CP 68525, Rio de Janeiro, RJ, 21945-970, Brazil; E-mail: mibt@ima.ufrj.br

matrix, because this method permits a better dispersion of the nanoparticles in the polymer matrix and also maintains some nanoparticles in the surface area that can act rapidly. Besides its characteristics as a good catalyst in the industry and corrosion-resistant alloys; its good characteristic as potential antimicrobial agent through the mechanism metal-metal oxide-polymer; which could generate a protection action; making nanocomposite active [22-24]. There are some studies on this theme to better understand the trioxide molybdenum characteristic action as anti-microbial and antiviral protection.

Thus, the main purpose of this work was to study the molecular dynamics, morphology, thermal stability and mechanical performance of nanomaterials formed by poly(vinyl alcohol) and molybdenum trioxide, obtained through solution method, to understand the materials behavior, focusing their dispersion and distribution mode in the polymer matrix and their antimicrobial characteristic to make possible antivirals act against COVID-19.

The obtained materials were characterized through the conventional techniques as X-ray diffraction, thermal analyses and dynamical-mechanical analysis. The low-field NMR relaxometry was employed to evaluate the molecular dynamic and the morphology of the new materials, through the intermolecular interaction forces and chains molecular organization, which will permit to infer about the materials morphology [19-25].

It is known that NMR relaxometry can evaluate the changes in the molecular mobility and can infer in the nanocomposite organization due to the evolution of proton spin-lattice relaxation time. This parameter is sensitive to the domain formation with size varied from 25 to 50 nm [25-30]. The organization of the polymer chains when lamellar nanoparticle is added in a polymer matrix can be evaluated from the changes in the proton spin-lattice values. An increase in this parameter may come from the intercalated structure, because the chains molecular mobility decreases when these chains are in between lamellae, due to the restriction in their molecular movement. By contrary, when the proton spin-lattice values decrease an exfoliated structure form is preferred due to the increase in the molecular mobility of polymer chains to move around the oxide lamellae and also the metal acts as a relaxing agent [19-29].

The systems focused in this work have never been studied yet, and their evaluation applying NMR

relaxometry has not been done before. Thus, the systems prepared and characterized by some specific techniques present a great novelty for the nanocomposites area, focusing on its potential antimicrobial [14] and possible antivirals action to avoid COVID-19.

EXPERIMENTAL

Materials

Poly(vinyl alcohol) (PVA) 88% hydrolyzed was supplied by VETEC Quimica Fina LTDA. Molybdenum trioxide (MoO_3) 99% was purchased from Merck KGaA and both chemicals were used as received.

PVA/ MoO_3 Films Preparation

The PVA/ MoO_3 films were prepared by the conventional solution casting method in which the polymer is solubilized in deionized water under magnetic stirring at 80 °C forming a solution of 5 wt.% (polymer/solvent). Molybdenum trioxide at concentration of 0.5, 1.0, 1.5, 2.0 and 2.5 wt.% (MoO_3 /polymer) was swelled in deionized water and sonicated for approximately 2 hours at 60 °C in a sonicator bath. Then, the solution was heated at 80 °C under magnetic stirring overnight. Partially hydrolyzed PVA was added to the mixture to prepare PVA/ MoO_3 /water mixture by total dissolution at 80 °C under magnetic stirring overnight too. Therefore, the solutions were poured in a Petri dish and dried at 50 °C. The membranes presented thickness values around 150 μm . The PVA/ MoO_3 composites films prepared with 0, 0.5, 1.0, 1.5, 2.0 and 2.5 wt.% of MoO_3 were named in this work as PM0, PM1, PM2, PM3, PM4 and PM5, respectively.

X-Ray Diffraction Measurements (XRD)

X-ray diffraction measurements were obtained using a Rigaku Miniflex II diffractometer, equipped with a Cu K α radiation source ($\lambda = 1,5418 \text{ \AA}$), operating at 40 kV and 100 mA. The scanning rate was $0.05^\circ \text{ s}^{-1}$ and the corresponding intensities were measured over a 2θ interval from 2 to 40°. Measurements have been performed at room temperature.

Thermogravimetric Analysis (TGA)

Thermogravimetric analysis was performed using a TA Instruments Q500 analyzer operating at a heating rate of 10 °C/min, under nitrogen atmosphere (balance gas: nitrogen 40.0 mL.min⁻¹ and sample gas: nitrogen

60.0 mL.min⁻¹). The TGA profiles were recorded in the temperature range from 30 up to 700 °C. The weight of the sample used was about 5–7 mg in all the cases.

Dynamic Mechanical Analysis (DMA)

Dynamic mechanical analyzer (Q-800, TA Scientific) was employed for performing dynamic mechanical properties of PVA/MoO₃ films at a fixed frequency of 1 Hz and oscillation amplitude of 0.15 mm. The measurements were carried out by heating from 30 to 170 °C under nitrogen atmosphere at a heating rate of 5 °C/min.

Solid-State ¹H Low-Field NMR Relaxometry

Proton Spin-Lattice Relaxation Time Measurements

To obtain information from the molecular dynamics of the PVA/MoO₃ composites, the spin-lattice relaxation times (T_{1H}) were determined by low-field NMR spectroscopy in the solid-state using a Maran Ultra 23 spectrometer (Resonance Instruments, Oxford, UK), operating at 23.4 MHz (for protons) and equipped with an 18 mm variable temperature probe. The pulse sequence used for T_{1H} determination was inversion-recovery (recycle delay 180° – τ – 90° acquisition). The 90° pulse, 4.7 μ s, was calibrated automatically by the instrument software. The amplitude of the free induced decay (FID) was sampled for 40 τ data points, ranging from 10 to 10⁶ ms, with four scans each and 5 s of recycle delay. All measurements were performed at 27 °C. The T_{1H} values and relative intensities were obtained by exponential fitting of available data with the aid of the WINFIT program. Distributed exponential plots of relaxation amplitude versus relaxation time were fitted by using the WINDXP software.

RESULTS AND DISCUSSION

X-Ray Diffraction Measurements

Figure 1 shows the X-ray diffraction pattern of the α -MoO₃ between $2\theta = 2^\circ$ and 40° . The diffraction peaks at $2\theta = 12.91^\circ$, 23.69° , 26.00° , 27.61° and 39.39° , correspond to the indices of (020), (110), (040), (021), and (060) planes of orthorhombic MoO₃ phase, respectively. The layered structure of MoO₃ with interlayer spacing around 6.9 Å can be observed from the (020) plane.

XRD patterns of the PVA/MoO₃ composites films with different amounts of MoO₃ are presented in Figure 2. From this Figure it was possible to observe the

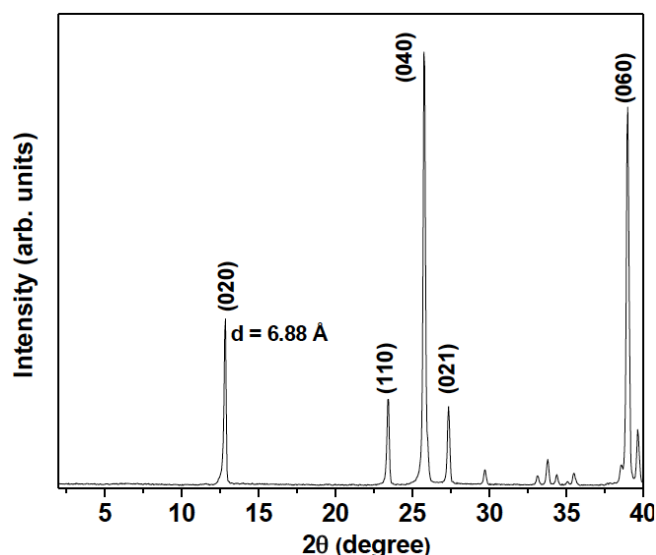


Figure 1: X-ray diffraction pattern of α -MoO₃.

peaks related to α -MoO₃ (020), (040) and (060), confirming the incorporation of the MoO₃ into PVA matrix. The pattern found for X-ray peaks are due to the MoO₃ architecture in the lamellae form that brings to this metal oxide their required properties, as antimicrobial effect, for example. This metal oxide was already used with the new material against H1N1 [14]. In this sense, we hope to use this new material against COVID-19.

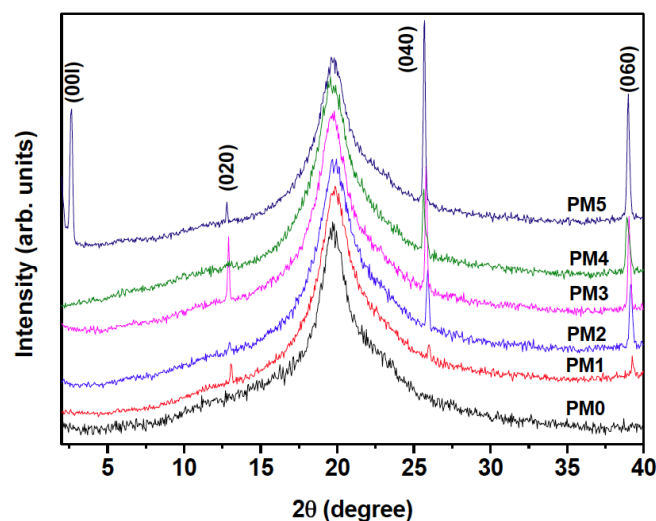


Figure 2: X-ray diffraction patterns of PVA and the corresponding PVA/MoO₃ based composite films.

An unexpected and sharp intense peak at lower angles for PM5 sample (2.5 wt.% of MoO₃) can be clearly seen from the XRD patterns (Figure 3). This peak was not found in others PVA/MoO₃ nanocomposites and pristine MoO₃. According to Bragg Law, this peak at $2\theta = 2.65^\circ$ is related to the

crystal plane (001) and corresponds to a d-spacing of 33.3 Å, which suggests the presence of poly(vinyl alcohol) chains between MoO₃ lamellae, leading to intercalated structure. This result shows that PVA film containing 2.5 wt. % of MoO₃ was the composite system that presents a more intercalated morphology.

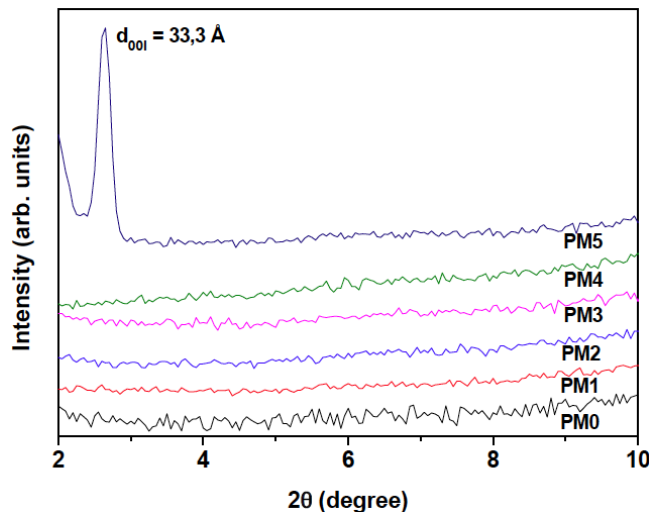


Figure 3: X-ray diffraction patterns of PVA and the corresponding PVA/MoO₃ films from $2\theta = 2^\circ$ to 10° .

Thermogravimetric Analysis

Thermal analysis is an important characterization that helps to direct the use of materials for specific applications. The thermal stability of the composite films (Figure 4) was evaluated by TGA under nitrogen atmosphere. From this Figure, it was possible to observe that the pattern of thermal degradation curves of the composites is different compared to the film without MoO₃. Table 1 exhibits the data of the thermal degradation for all systems studied, showing the initial degradation temperature (T_d onset) and the correlation of the temperature found when the mass lost corresponded to 5, 10 and 50 % (T_{d5} , T_{d10} and T_{d50} , respectively).

According to TGA results showed in the Table 1, the addition of MoO₃ into PVA matrix caused a slight and progressive reduction in the T_d onset. It was possible due to hydroxyl groups loss in different sites of the PVA chains. On the other hand, it was seen that at higher temperatures, an improvement in thermal stability was observed, due to lamellar structure of MoO₃. It was seen for example, that T_{d50} (temperature at which 50 wt.% of the mass is degraded) was displaced to higher temperatures for all composite films. The system containing a higher MoO₃ proportion (PM5) presented the most significant result with an increase of 56 °C in

the temperature to degrade 50 wt.% of the total mass. This effect was possibly promoted for morphological change in the PVA matrix by MoO₃ addition and occurs because lamellar structures tend to form physical barriers during the release of volatiles which may result in improvement on the thermal stability of the polymer matrices. This result corroborates to that found by XRD analysis that showed a more significant morphological change for PM5 system.

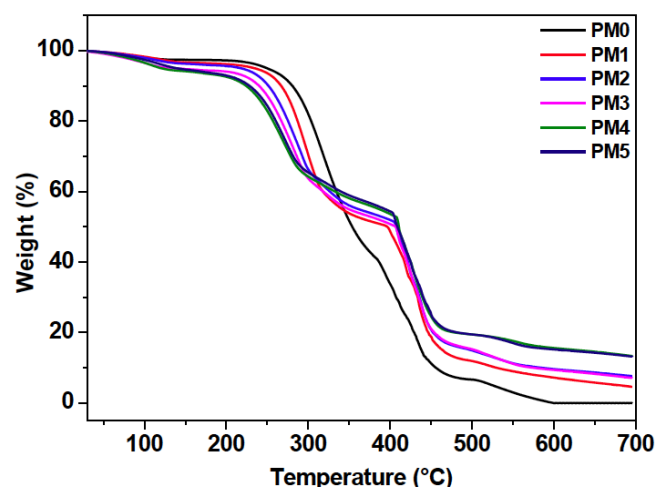


Figure 4: TGA curve showing the thermal stability of the PVA pristine and their composite films containing different MoO₃ proportions.

Table 1: Thermal Degradation Data for all PVA/MoO₃ Systems Produced

Samples	T_d onset	T_{d5} (°C)	T_{d10} (°C)	T_{d50} (°C)
PM0	279	251	281	353
PM1	267	236	267	396
PM2	250	214	251	407
PM3	243	140	240	406
PM4	231	118	223	411
PM5	236	135	228	409

Dynamic Mechanical Analysis (DMA)

DMA was carried out by applying a sinusoidally varying force to samples to measure the viscoelastic behavior of the PVA/MoO₃ systems investigated.

The curves obtained from the dynamic mechanical analysis of the composites systems are showed in the Figure 5, which compares the variation of the storage module, E' , with the increase in temperature for the different composites investigated. It was clearly seen that up to a certain temperature (70 °C) the values of E' found for all the composites were superior to that of

pure PVA, ie 0wt.% of MoO₃ (PM0), revealing a higher rigidity for all PVA/MoO₃ systems. The E' values found at 30 °C (at room temperature) were 128 MPa, 149 MPa, 155 MPa, 162 MPa, 690 MPa and 1020 MPa for the PM0, PM1, PM2, PM3, PM4 and PM5, respectively, being significantly higher for composites PM4 and PM5 that contain higher MoO₃ proportion (2.0 and 2.5 wt.%, respectively). Compared to the PVA without MoO₃ (PM0), the increase in the E' values for PM4 and PM5 were approximately 540% and 800%, respectively. The value of E' is directly related to the capacity of the material withstand mechanical loads with recoverable viscoelastic deformation. So higher E' means a more rigid structure for the investigated composites, thus the composite system that presented the greatest rigidity was PVA containing 2.5wt.% of MoO₃.

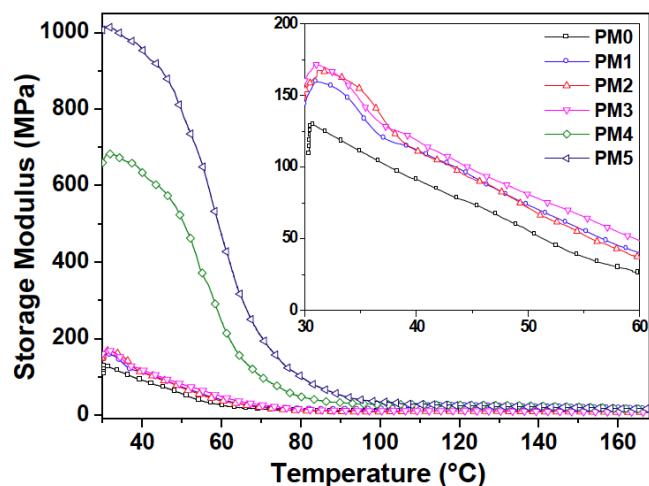


Figure 5: Curves of the dynamic mechanical analysis of the systems – storage modulus.

The glass transition (T_g) data obtained from tan Delta results reveal that for all nanocomposites films, the T_g values were higher compared to the PVA without MoO₃ (PM0). The T_g values found were 62.3 °C, 74.0 °C, 76.2 °C, 70.5 °C, 87.2 °C and 92.6 °C for PM0, PM1, PM2, PM3, PM4 and PM5, respectively. This result shows a tendency to increase the T_g value with the progressive addition of MoO₃ and confirms a change in the organization profile of the composites films as revealed by E' results that showed an increase in the rigidity of the PVA/MoO₃ systems. This result also suggests a strong interaction between PVA matrix and MoO₃ filler, showing that the presence of MoO₃ caused morphological change in the PVA matrix.

NMR Relaxometry Study

Figure 6 shows the domain curves obtained from proton spin-lattice relaxation time of PVA and

PVA/MoO₃ systems. Analyzing PVA pristine (PM0) domain curves, the area curve is large, which is derived from a heterogeneous material, since this polymer present amorphous and organized region. Both PM1 and PM2 systems showed a more uniform domain curves after the incorporation of molybdenum oxide in the polymer matrix, due to a better dispersion and distribution of the nanoparticles in the polymer matrix in both regions, generating a more homogeneous material. The nanoparticle incorporation promoted a decreased effect anisotropic dipolar present in the polymer. For the other three compositions, it was observed a different behavior. They showed to be more heterogeneous, formed by both morphology (exfoliated and intercalated) and the domain curves become large in the base for the three highest MoO₃ proportion, mainly evidenced for PM5 that showed to be one system containing a high degree of intercalated morphology. The enlargement of the area curve is the result of dipolar interactions generated by H and OH, suggesting a formation of materials containing different populations of hydrogen that relax differently due to these samples organization. Generally speaking, as greater are the interaction forces, greater is the enlargement.

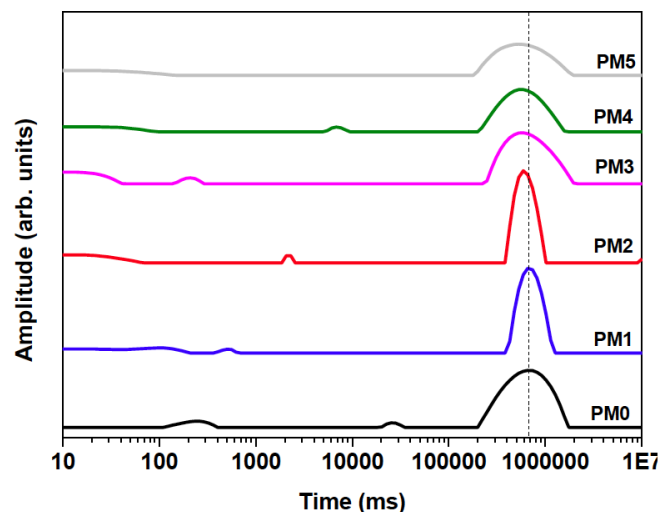


Figure 6: Domain curves of PVA pristine and PVA/MoO₃ systems.

Table 2 exhibits the values of the proton spin-lattice relaxation parameter, with a time constant (T₁H), these values were determined from the domains curves for all systems. PM1 and PM2 showed values of T₁H higher than the PM0, showing that the values of T₁H average time has a contribution of rigid domain, that controls to the relaxation data and it is predominating, since these samples are more homogenous. This behavior comes from the contribution the collective molecular

movement of the chains [27-30]. As the oxide is added to a polymer, it interacts with the H of hydroxyl leading to a decrease effect in the anisotropic dipolar interactions, present in the polymer, indicating that novel intermolecular interactions are formed. Analyzing PM3 it is in the transition of PM1 and PM2 and PM4 and PM5, showing its own behavior. PM3, PM4 and PM5 present two domains, but the rigid domain is more predominant, comparing to amorphous phase. For the systems PM4 and PM5, the values of relaxation decreased a little comparing to PVA pristine, which comes from the changes in the intermolecular interactions that affects the freedom of the molecular chains movement; showing that when MoO₃ is added in higher proportions, multiple interactions occur due to intercalation of the oxide among the polymer chains. Given more molecular freedom for the polymer chains to move, which caused a decrease of the relaxation value. These results indicate that both systems are heterogenous containing at least two domains with different molecular mobility. Therefore, all systems presented good intermolecular interaction between polymer and MoO₃ particle. As this metal oxide presents lamellar structure it can be seen that samples named from PM1 to PM3 presented a predominance of polymer chains in the oxide lamellae, because the relaxations data are higher than the polymer itself; which promotes the diminish of the molecular collective movement being restricted, and PM4 and PM5 showed a more exfoliated oxide lamellae along the polymer matrix, since the relaxation values present some decrease.

Table 2: Proton Spin-Lattice Relaxation Time

Samples	T ₁ H (ms)
PM0	580
PM1	673
PM2	621
PM3	591
PM4	534
PM5	544

CONCLUSIONS

The new materials prepared showed a singular behavior due to their new characteristics after MoO₃ being incorporated into PVA matrix, showing a good dispersion in this polymer matrix using the solution casting method.

All techniques used to characterize the properties of the new materials allowed us to evaluate the new

characteristics of the systems obtained. XRD confirmed the MoO₃ incorporation for all systems and showed that PM5 has a more intercalated morphology. TGA showed that all systems increased the thermal stability at higher temperatures. DMA showed that the progressive MoO₃ addition leads to increase on the rigidity of the systems. We could also note that the NMR relaxometry was a particularly good technique to evaluate the morphology at molecular level of the systems, showing that the all systems presented good PVA/MoO₃ intermolecular interaction and that lower MoO₃ proportion promote more homogeneous systems.

REFERENCES

- [1] Lackner M, Maninger S, Guggenbichler JP. *Nachr Chem* 2013; 61: 112-115. <https://doi.org/10.1002/nadc.201390038>
- [2] Lackner M, Guggenbichler JP. Patent DE102011085862. 2013.
- [3] Lackner M, Guggenbichler JP. Patent DE102012103064. 2013.
- [4] Guggenbichler JP, Eberhardt N, Martinez HP, Wildner H. Patent US20100057199. 2010.
- [5] Shafaei S, Opendbosch DV, Fey T, Koch M, Kraus T, Guggenbichler JP, Zollfrank C. *Materials Science and Engineering C* 2016; 58: 1064-1070. <https://doi.org/10.1016/j.msec.2015.09.069>
- [6] Bechert T, Steinrucke P, Guggenbichler JP. *Nat Med* 2000; 6: 1053-1056. <https://doi.org/10.1038/79568>
- [7] Kalaycı OA, Comert FB, Hazer B, Atalay T, Cavicchi KA, Cakmak M. *Polym Bull* 2010; 5: 215-226. <https://doi.org/10.1007/s00289-009-0196-y>
- [8] Delgado K, Quijada R, Palma R, Palza H. *Lett Appl Microbiol* 2011; 53: 50-54. <https://doi.org/10.1111/j.1472-765X.2011.03069.x>
- [9] Raghupathi KR, Koodali RT, Manna AC. *Langmuir* 2011; 27: 4020-4028. <https://doi.org/10.1021/la104825u>
- [10] Hazer DB, Burcu D, Mut M, Dincer N, Saribas Z, Hazer B, Ozgen T. *Childs Nerv Syst* 2012; 28: 839-846. <https://doi.org/10.1007/s00381-012-1729-5>
- [11] Das D, Nath BC, Phukon P, Dolu SK. *Colloids Surf B Biointerfaces* 2013; 101: 430-433. <https://doi.org/10.1016/j.colsurfb.2012.07.002>
- [12] Lackner M, Maninger S, Guggenbichler JP. *Nachr Chem* 2013; 61: 112-115. <https://doi.org/10.1002/nadc.201390038>
- [13] Shafaei S, Lackner M, Voloshchuck R, Voloshchuck I, Guggenbichler JP, Zollfrank C. *Recent Patents Mater Sci* 2014; 7: 26-36. <https://doi.org/10.2174/1874464806666131204235326>
- [14] Shafaei S, Dorrstein J, Guggenbichler JP, Zollfrank C. *Letters in Applied Microbiology* 2016; 64: 43-50. <https://doi.org/10.1111/lam.12670>
- [15] Iulianelli GCV, David G, dos S, Santos TN, Sebastião PJO, Tavares MIB. *Polymer Testing* 2018; 65: 156-162. <https://doi.org/10.1016/j.polymertesting.2017.11.018>
- [16] Brito LM, Tavares MIB. *Journal of Nanoscience and Nanotechnology* 2012; 12: 1-6. <https://doi.org/10.1166/jnn.2012.6176>

- [17] Almeida AS, Tavares MIB, Silva EO. *Polymer Testing* 2012; 31: 267-275.
<https://doi.org/10.1016/j.polymertesting.2011.11.005>
- [18] Nogueira RF, Tavares MIB, Ferreira AG. *Journal of Nanoparticle Research* 2012; 1026-1034.
- [19] Monteiro MSSB, da Silva EO, Rodrigues CL, Neto RPC, Tavares MIB. *Journal of Nanoscience and Nanotechnology* 2012; 12: 7307-7313.
<https://doi.org/10.1166/jnn.2012.6431>
- [20] Monteiro MSSB, Neto RPC, Santos ICS, da Silva EO, Tavares MIB. *Materials Research* 2012; 15: n5.
<https://doi.org/10.1590/S1516-14392012005000121>
- [21] Soares IP, Chimanowsky JP, Luetkmeyer L, da Silva EO, Souza DHS, Tavares MIB. *Journal of Nanoscience and Nanotechnology* 2015; 15: 5723-5732.
<https://doi.org/10.1166/jnn.2015.10041>
- [22] Qureshi N, Chaudhari R, Mane P, Shinde M, Jadakar S, Rane S, Kale B, Bhalerao A, Amalnerkar D. *EEE Trans Nanobioscience* 2016; 15: 258-264.
<https://doi.org/10.1109/TNB.2016.2535285>
- [23] Krishnamoorthy K, Veerapandian M, Yun K, Kim SJ. *Colloids Surf B Biointerfaces* 2013; 112: 521-524.
<https://doi.org/10.1016/j.colsurfb.2013.08.026>
- [24] Lopes E, Piçarra S, Almeida PL, de Lencastre H, Aires-de-Sousa M. *J Med Microbiol* 2018; 67: 1042-1046.
<https://doi.org/10.1099/jmm.0.000789>
- [25] Vanderhart DE, Asano A, Gilman JW. *Chemical Material* 2001; 13: 3796-3809.
<https://doi.org/10.1021/cm011078x>
- [26] Brito LM, Chávez FV, Tavares MIB, Sebastião PJO. *Polymer Testing* 2013; 32: 1181-1185.
<https://doi.org/10.1016/j.polymertesting.2013.07.002>
- [27] Bovey FA, Mirau PA. *NMR of Polymers*. Academic Press 1996.
- [28] Komorosky RA. *High resolution NMR spectroscopy of synthetic polymers in bulk*. VCH Publishers 1986.
- [29] Almeida DBR, Tavares MIB. *Materials Science and Applications* 2019; 10: 768-782.
<https://doi.org/10.4236/msa.2019.1012056>
- [30] Cecci R, Passos AA, Albino NRV, Silva VD, Duarte AS, Tavares MIB. *Journal of Materials Science and Engineering B* 2020; 10: 53-63.

Received on 01-12-2020

Accepted on 26-12-2020

Published on 30-12-2020

DOI: <https://doi.org/10.6000/1929-5995.2020.09.09>© 2020 Tavares *et al.*; Licensee Lifescience Global.

This is an open access article licensed under the terms of the Creative Commons Attribution Non-Commercial License (<http://creativecommons.org/licenses/by-nc/3.0/>) which permits unrestricted, non-commercial use, distribution and reproduction in any medium, provided the work is properly cited.